ELSEVIER

Biophysical Chemistry 74 (1998) 197–207

Biophysical Chemistry

Coexistence of multiple propagating wave-fronts in a regulated enzyme reaction model: link with birhythmicity and multi-threshold excitability

C. Pérez-Iratxeta[a,1], J. Halloy[b], F. Morán[a], J.L. Martiel[c], A. Goldbeter[b,*]

[a] *Departamento de Bioquimica, Faculdad de Quimicas, Universidad Complutense, E-28040 Madrid, Spain*
[b] *Faculté des Sciences, Université Libre de Bruxelles, Campus Plaine, C.P. 231, B-1050 Brussels, Belgium*
[c] *Département d'Informatique Médicale, Faculté de Médecine, Université de Grenoble, F-38700 La Tronche, France*

Received 27 May 1998; received in revised form 23 June 1998; accepted 25 June 1998

Abstract

We analyze the spatial propagation of wave-fronts in a biochemical model for a product-activated enzyme reaction with non-linear recycling of product into substrate. This model was previously studied as a prototype for the coexistence of two distinct types of periodic oscillations (birhythmicity). The system is initially in a stable steady state characterized by the property of multi-threshold excitability, by which it is capable of amplifying in a pulsatory manner perturbations exceeding two distinct thresholds. In such conditions, when the effect of diffusion is taken into account, two distinct wave-fronts are shown to propagate in space, with distinct amplitudes and velocities, for the same set of parameter values, depending on the magnitude of the initial perturbation. Such a multiplicity of propagating wave-fronts represents a new type of coexistence of multiple modes of dynamic behavior, besides the coexistence involving, under spatially homogeneous conditions, multiple steady states, multiple periodic regimes, or a combination of steady and periodic regimes.

Keywords: Excitability; Oscillations; Birhythmicity; Reaction-diffusion; Waves

* Corresponding author. Tel.: +32 2 6505772; fax: +32 2 6505767; e-mail: agoldbet@ulb.ac.be
[1] Present address: Protein Design Group, CNB/CSIC, Campus UAM, 28049 Cantoblanco, Madrid, Spain.

0301-4622/98/$19.00
PII S0301-4622(98)00179-3

1. Introduction

The coexistence between multiple, simultaneously stable modes of dynamic behavior is a characteristic property of non-linear systems in chemistry, physics and biology [1]. Under spatially homogeneous conditions, such a coexistence can take different forms. The most common type of coexistence is that of bistability, in which the system can reach either one of two steady states which are stable under the same conditions, i.e. for a given set of parameter values. Several cases of such bistability are known experimentally in biochemistry, one of the first examples being that of the peroxidase reaction [2]. Tristability, involving the coexistence of three stable steady states, is also known [3]. The phenomenon can in principle be extended to involve even more stable steady states, although the domain in parameter space where such a multiplicity occurs is likely to become smaller and smaller as the number of simultaneously stable states increases.

Another mode of coexistence, known as hard excitation [4], refers to the evolution towards either a steady state or a regime of sustained oscillations of the limit cycle type, which are stable under the same conditions. Several examples of hard excitation are known, from a theoretical and experimental point of view; to restrict the discussion to biological systems, the phenomenon has been demonstrated in neurobiology [5] and in a cardiac preparation [6]. Finally, a third type of coexistence is that of birhythmicity [7,8], which is the rhythmic counterpart of bistability: two regimes of sustained oscillations of the limit cycle type may coexist for a given set of parameter values. The phenomenon has not yet been observed experimentally in biological systems, but its occurrence in chemical oscillatory reactions was demonstrated in a number of cases [9–11] after its theoretical prediction in a model for a multiply regulated biochemical system [7]. The coexistence between three (trirhythmicity) or more distinct periodic regimes is also known theoretically [12–14] but, as with multiple steady states, the phenomenon becomes more rare as the number of coexisting rhythms increases.

The conditions for the occurrence of birhythmicity were clarified thanks to the analysis of a two-variable biochemical model which permitted to verify a conjecture for the origin of the phenomenon, based on phase plane analysis [15]. The same model allowed the characterization of the closely related phenomenon of multi-threshold excitability: whereas oscillatory systems generally display the property of excitability, by which they are capable of amplifying in a pulsatory manner a perturbation exceeding a threshold, two distinct thresholds are observed in the model admitting birhythmicity [16].

Systems which display temporal organization in the form of sustained oscillations of the limit cycle type are also capable to self-organize in space and to display stable spatial patterns of the Turing type, or spatiotemporal structures in the form of propagating concentration waves [1]. The phenomenon has been studied in detail in chemical oscillatory systems, such as the Belousov–Zhabotinsky reaction [17], and is illustrated experimentally in biochemical systems by oscillations and waves of intracellular Ca^{2+} [18–20] and cyclic AMP waves in aggregating *Dictyostelium* amoebae [21].

Much less is known about the coexistence of multiple stable patterns of spatial or spatiotemporal organization than about bistability, birhythmicity or hard excitation. Indeed, the study of the occurrence of multiple stable solutions in chemical or biological systems has mainly been restricted to homogeneous conditions. The purpose of the present paper is to provide an example of a multiplicity of spatiotemporal patterns, by using the two-variable model previously analyzed for birhythmicity. When incorporating the effect of diffusion into this biochemical model we show, by means of numerical simulations, the coexistence between two different types of propagating wave-fronts. The selection of either one of these wave-fronts depends on the amplitude of the initial perturbation of the homogeneous, excitable steady state.

2. Model and kinetic equations

The two-variable model considered for birhythmicity [15] and multi-threshold excitability

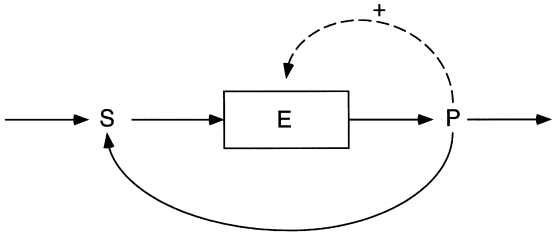

Fig. 1. Biochemical model of a product-activated enzyme reaction with non-linear recycling of product into substrate. This two-variable model, capable of birhythmicity and multi-threshold excitability (see Morán and Goldbeter [15,16] and also Goldbeter [8]), is used here to demonstrate the possibility of a coexistence between two distinct wave-fronts, depending on the magnitude of the initial perturbation.

[16] is schematized in Fig. 1. It represents an enzymatic reaction in which the substrate, S, injected at a constant rate, is transformed into a product, P, which activates the allosteric enzyme, E, that catalyzes the transformation of S into P. Moreover, the product is recycled into substrate by a second reaction catalyzed by an enzyme whose cooperative kinetics is described by a Hill equation, characterized by a degree of cooperativity n. In the absence of recycling, the product-activated enzyme model accounts for sustained glycolytic oscillations in yeast and muscle [8,22]. In the presence of recycling, the system acquires the properties of birhythmicity [15] and multi-threshold excitability [16] (see also Goldbeter [8]).

The kinetic equations of the model thus take the form [8,15,16]:

$$\frac{\mathrm{d}\alpha}{\mathrm{d}t} = v + \frac{\sigma_i \gamma^n}{K^n + \gamma^n} - \sigma\phi$$

$$\frac{\mathrm{d}\gamma}{\mathrm{d}t} = q\sigma\phi - k_s\gamma - \frac{q\sigma_i \gamma^n}{K^n + \gamma^n} \qquad (1)$$

In the above equations, α and γ denote the concentrations of substrate and product normalized, respectively, by division by the Michaelis constant of the product-activated enzyme (K_m) and by the dissociation constant of the product for the regulatory site of this enzyme (K_P); v and σ denote, respectively, the normalized substrate input and the maximum rate of the product-activated enzyme reaction; $q = K_m/K_P$; k_s is the apparent first-order rate constant for removal of product; parameter σ_i denotes the normalized maximum rate of recycling of product into substrate; constant K is equal to the product concentration for which the recycling rate reaches its half-maximum value. The rate function ϕ of the product-activated allosteric enzyme, in the case of a dimeric enzyme that binds the substrate only in the active state, takes the simple form:

$$\phi = \frac{\alpha(1+\alpha)(1+\gamma)^2}{L + (1+\alpha)^2(1+\gamma)^2} \qquad (2)$$

where L denotes the allosteric constant of the enzyme (see Goldbeter [8] and [15] for further details on the equations and on the definition of parameters).

When diffusion of substrate and product is taken into account, Eq. (2) takes the form:

$$\frac{\partial\alpha}{\partial t} = v + \frac{\sigma_i \gamma^n}{K^n + \gamma^n} - \sigma\phi + D_\alpha \frac{\partial^2\alpha}{\partial r^2}$$

$$\frac{\partial\gamma}{\partial t} = q\sigma\phi - k_s\gamma - \frac{q\sigma_i \gamma^n}{K^n + \gamma^n} + D_\gamma \frac{\partial^2\gamma}{\partial r^2} \qquad (3)$$

where D_α and D_γ denote the diffusion coefficients of substrate and product, respectively. In the following numerical simulations, given that it is the product that triggers the excitable response, we will consider, for simplicity, the case where only the product is diffusing ($D_\alpha = 0$). We have checked that the results do not change significantly when D_α is less than D_γ by one order of magnitude.

3. Coexistence of two propagating wave-fronts

To demonstrate the coexistence of two propagating wave-fronts, we first consider the behavior of the homogeneous system described by Eq. (1), to specify the reference state that shall be taken as initial condition in the simulations of the spatiotemporal evolution based on integration of Eq. (3).

The reference state to be considered is one in which the system displays the property of multi-threshold excitability [16]. In such a state (see Fig.

2a), the system is capable of amplifying in a pulsatory manner perturbations that exceed two distinct thresholds, giving rise to a small and a large peak of synthesis of the reaction product, respectively, before the system returns to the stable steady state located at the intersection of the two nullclines (black dot in Fig. 2b). The phase plane trajectories associated with these excitable responses are shown in Fig. 2b, together with the nullclines $d\alpha/dt = 0$ and $d\gamma/dt = 0$ obtained by setting the right-hand side of Eq. (1) equal to zero.

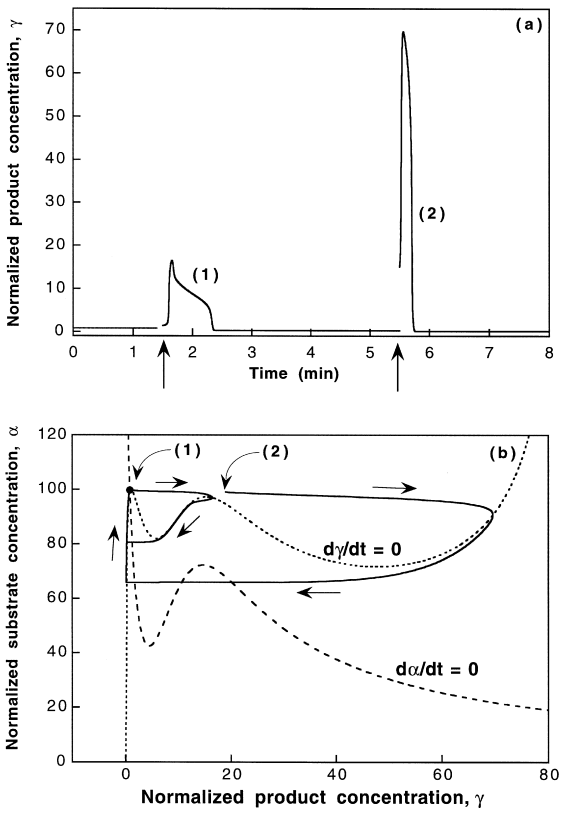

Fig. 2. Dynamic behavior of the model of Fig. 1 under spatially homogeneous conditions. The model illustrates the effect of two instantaneous increases in the product concentration, exceeding the first and second threshold for excitability. (a) Time evolution obtained by integration of Eq. (1); (b) phase plane portrait, showing the nullclines for the substrate (dotted line) and product (dashed line), and the trajectories corresponding to the time evolution shown in (a) in response to the two stimuli of increasing magnitude. The arrows marked (1) and (2) in (a) and (b) indicate the perturbations in the form of instantaneous increases in product concentration away from the steady state ($\alpha = 99.645$, $\gamma = 0.8$), up to the values $\gamma = 1.4$ for (1) and $\gamma = 15$ for (2) (the latter initial value has been chosen for the sake of clarity, to distinguish between the two trajectories, even though a smaller initial value of γ, above the second threshold close to 1.6, would also produce a large-amplitude excursion in the phase plane). In (b) the steady state is represented by a dot at the intersection of the two nullclines; the arrows along the trajectories indicate the direction of movement in the phase plane following the perturbations in γ. Parameter values are: $v = 0.04\ s^{-1}$, $\sigma = 6.2\ s^{-1}$, $n = 4$, $q = 60$, $k_s = 3\ s^{-1}$, $L = 5 \times 10^6$, $\sigma_i = 2\ s^{-1}$, $K = 13$.

As explained in Morán and Goldbeter [16], the property of multi-threshold excitability is associated with the existence of a second region of negative slope $(d\alpha/d\gamma)$ on the product nullcline $d\gamma/dt = 0$. The phenomenon was previously analyzed in conditions where the second region of negative slope rises above the horizontal through the steady state [16]. The existence of two distinct thresholds can readily be demonstrated in such conditions. Here, although the second region of negative slope is located slightly below this horizontal line, two thresholds for excitability can nevertheless be observed, as shown in Fig. 2b. The first threshold, in the case considered, is close to $\gamma = 1.3$, while the second threshold is close to $\gamma = 1.6$. Because the first threshold is so close to the steady state (which lies in $\gamma = 0.8$) on the scale of Fig. 2b, the initial displacement up to $\gamma = 1.4$ for trajectory (1) is not clearly visible (see also Fig. 2a).

In the case of Fig. 2b, the substrate nullcline also possesses a local maximum and the trajectory (2) crosses the nullcline three times on its return to the left limb of the nullcline after generating the peak in γ. We have verified that the sign of $(d\alpha/dt)$ changes as expected from these multiple crossings of the nullcline; these variations, however, are so minute that they do not lead to any visible changes in the trajectory which seems to retain the same sign for $(d\alpha/dt)$ all along in that region.

Turning to the spatiotemporal evolution described by Eq. (3) in the presence of diffusion, we consider that the system is initially in a stable steady state corresponding to the situation described in Fig. 2. Then, the steady state is stable but displays the property of multi-threshold excitability. When a suprathreshold, inhomoge-

neous perturbation is applied to the system initially in such a state, a single wave-front is seen to propagate from the site of stimulation. Two distinct types of wave-front, however, can be seen to propagate, depending on the amplitude of the perturbation, which consists in an instantaneous increase in the product concentration.

Values of the perturbation larger than the smaller threshold and less than the higher threshold in Fig. 2b trigger the propagation of a small-amplitude wave-front. The propagation phenomenon corresponding to such intermediate perturbations is represented in Figs. 3 and 4a along a single spatial dimension. In Fig. 3a, the time evolution of the product concentration in different points of the spatially extended system is shown, whereas in Fig. 4a the spatiotemporal evolution is represented for the entire one-dimensional system, in conditions where the suprathreshold perturbation of intermediate magnitude is applied to the left extremity of the system in a transient manner. The corresponding simulations over two spatial dimensions are shown in Fig. 5a–c in conditions where a similar perturbation is applied in the center of the system.

The corresponding effects of a larger perturbation exceeding the second threshold for excitability are shown in one (Figs. 3 and 4b) and two dimensions (Fig. 6a–c), respectively. Here, we see that such a perturbation elicits the propagation of a wave-front of large amplitude. It is important to stress that the small-amplitude and large-amplitude wave-fronts are obtained under the same conditions, i.e. for the same set of parameter values. The only difference pertains to the initial conditions, i.e. the value of the initial increase in the product concentration in the point of stimulation.

The two coexisting wave-fronts differ not only by the amplitude but also by the speed at which they propagate. Thus, as can be seen from the comparison of Fig. 3a,b, the high-amplitude wave-front propagates at a rate of approx. 0.15 cm/min, which is larger by some 7% than the rate of 0.14 cm/min at which the small-amplitude wave-front moves. Such values for the propagation rate are larger by a factor close to 2 than the wave propagation rate computed for other parameter values in this model in the absence of product recycling [23]. The propagation rate of the small-amplitude and the high-amplitude wave-fronts in two dimensions computed from Figs. 5 and 6 for a fivefold larger value of the product diffusion coefficient is, respectively, 0.16 and 0.18 cm/min. Again we observe that the rate of propagation of the high-amplitude front is larger by approx. 10% than the rate at which the small-amplitude front progresses in space.

What happens when two wave-fronts collide is shown by the simulations carried along a single spatial dimension in Fig. 7. In part (a) two wave-fronts of similar, small amplitude started at the two extremities of the system annihilate each other when they collide, after producing a single large-amplitude pulse due to the accumulation of product in the point of collision. A similar result is obtained when two wave-fronts of large amplitude meet in similar conditions [part (b)]. Mutual annihilation is also observed when a small-amplitude wave-front started at one extremity collides with a large-amplitude front initiated at the other extremity of the system [part (c)].

4. Discussion

We have shown that two wave-fronts of distinct amplitudes and velocities may propagate along one or two spatial dimensions, depending on the magnitude of the initial perturbation of the homogeneous steady state. The results were obtained in a two-variable biochemical model previously studied for birhythmicity and multi-threshold excitability, when taking into account the effect of diffusion in describing the time evolution of the system. The coexistence between two types of wave-fronts under given conditions, i.e for the same set of parameter values, illustrates a new type of coexistence of multiple modes of dynamic behavior in non-linear systems. Such a coexistence between two different wave-fronts is a direct consequence of the occurrence of birhythmicity and the related phenomenon of multi-threshold excitability in that system under spatially homogeneous conditions.

So far the coexistence of distinct modes of dynamic behavior has primarily been investigated

in spatially homogeneous conditions; numerous examples of such phenomena have been reported, both theoretically and experimentally. In such conditions, the coexistence pertains to two (or more) distinct stable steady states, one steady state and one periodic regime, or two (or more)

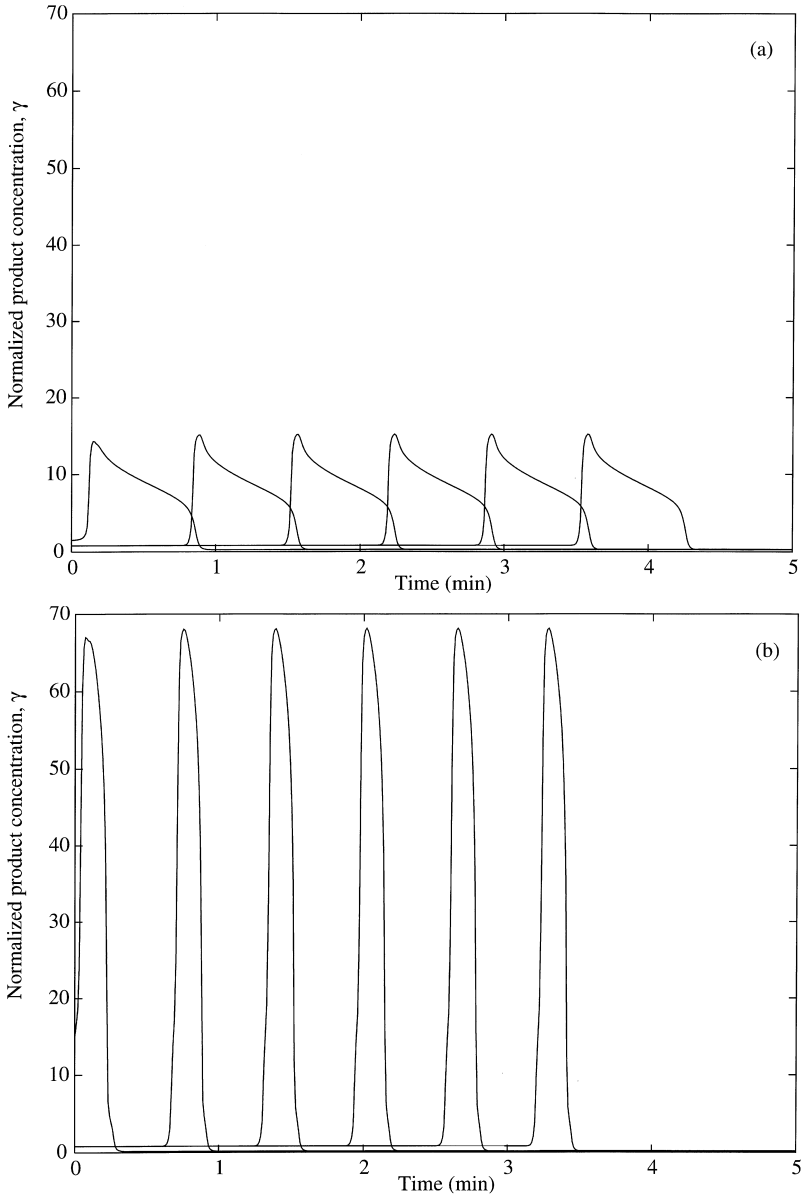

Fig. 3. Coexistence of two wave-fronts propagating along a single spatial dimension. Shown is the propagation of a small-amplitude (a) and a large-amplitude (b) wave-front. Space is represented by a mesh of 100 points. The curves show the time evolution of the normalized product concentration at points 1, 10, 20, 30, 40 and 50, successively. The curves are obtained by numerical integration of Eq. (3) for the parameter values of Fig. 2; moreover, $D_\gamma = 4 \times 10^{-5}$ cm^2/min, $D_\alpha = 0$. Initial conditions correspond to the homogeneous steady state $\alpha = 99.645$ and $\gamma = 0.8$, except at point 1 of the spatial mesh where $\gamma = 1.5$ for (a) and 15 for (b), initially. Boundary conditions are of the zero-flux type. The spatial dimension of the system is 1 cm.

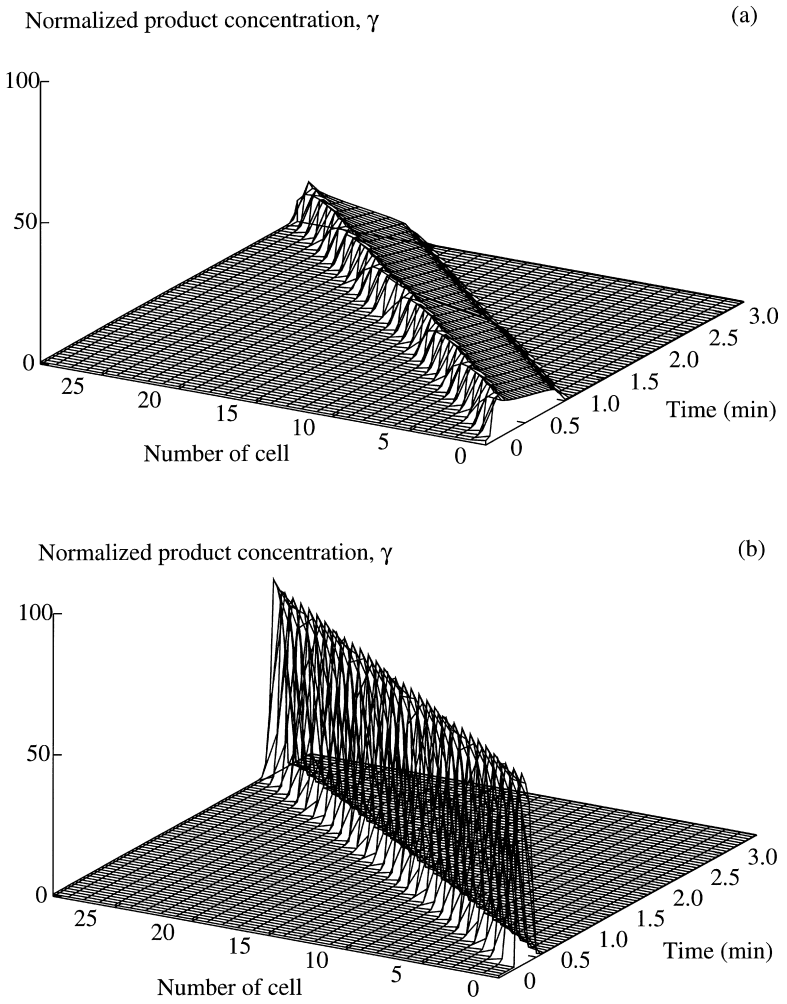

Fig. 4. Coexistence of two wave-fronts propagating along a single spatial dimension. Shown as a function of time and space is the propagation of a small-amplitude (a) and a large-amplitude (b) wave-front, in the conditions of Fig. 2. Simulations are performed using a spatial mesh of 30 points.

stable periodic regimes. The present study extends the study of coexisting modes of dynamic behavior to spatially inhomogeneous conditions. The coexistence of multiple stable spatial structures has previously been reported for a theoretical model for pattern formation [24]. As shown by a theoretical study of a reaction-diffusion model admitting two stable steady states [25], coexisting propagating waves might also originate from the coupling of diffusion with bistability instead of birhythmicity, as considered here.

The propagation phenomenon demonstrated in Figs. 3–7 is only transient, because the perturbation that triggers it is only applied at time zero. As in a model for oscillations and waves of intracellular Ca^{2+} [20], the wavelike phenomenon should become sustained when the perturbation is maintained at the appropriate level in the course of time.

From an experimental point of view, it would be interesting to test for the multiplicity of propagating wave-fronts in chemical systems. The best candidates for such a study would be the chemical oscillatory systems for which birhythmicity has

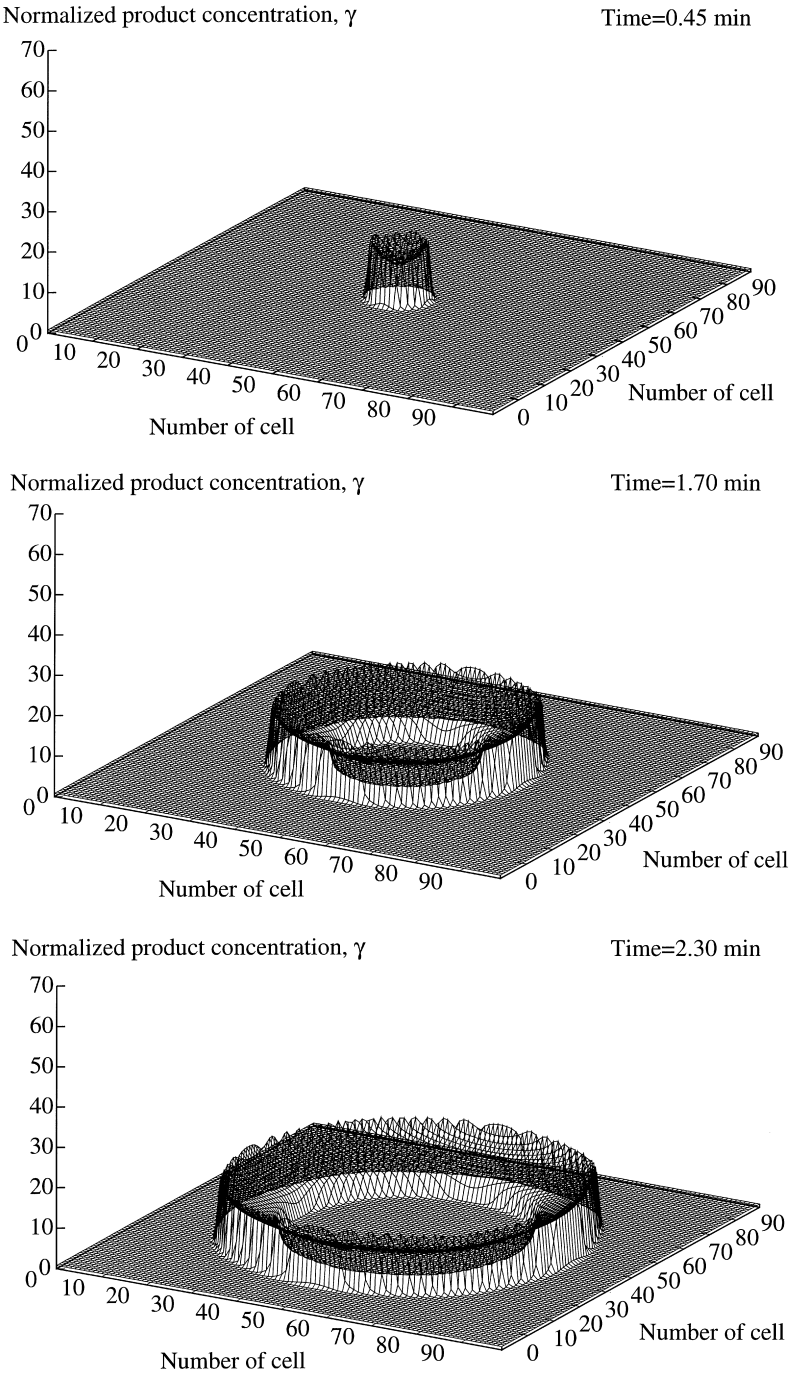

Fig. 5. Propagation of a small-amplitude wave-front in two spatial dimensions. The spatial distribution of the normalized product concentration, shown at three successive moments in time, is obtained by numerical integration of Eq. (3) for the parameter values of Fig. 3, with $D_\gamma = 2 \times 10^{-4}$ cm^2/min. Initial conditions correspond to the homogeneous steady state, except at the center point (50, 50) of the mesh of 100×100 points where $\gamma = 1.5$ initially. Boundary conditions are of the zero-flux type. The spatial dimensions of the system are 1 cm $\times$ 1 cm.

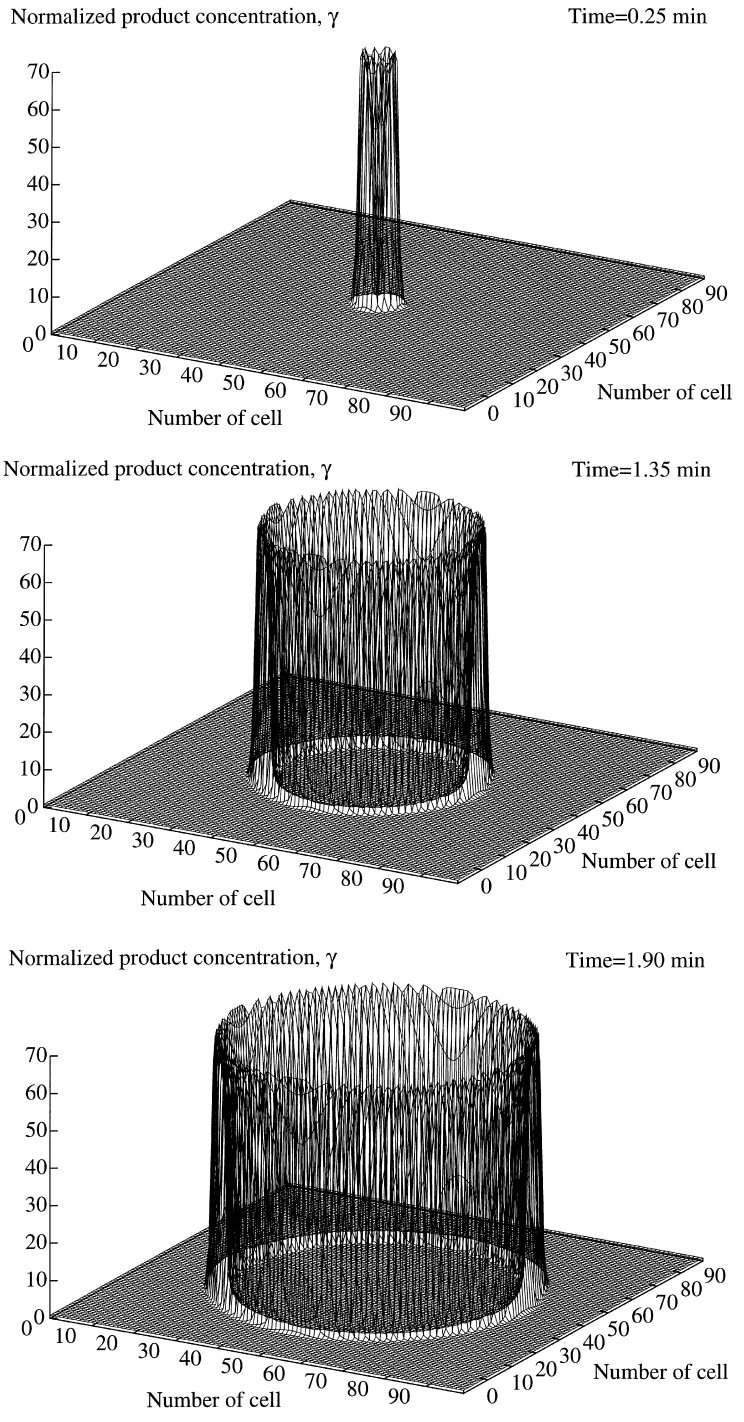

Fig. 6. Propagation of a large-amplitude wave-front in two spatial dimensions, in the same conditions as in Fig. 5. The spatial distribution of the normalized product concentration, shown at three successive moments in time, is obtained by numerical integration of Eq. (3) for the parameter values and boundary conditions of Fig. 5. Initial conditions correspond to the homogeneous steady state, except at the center point (50, 50) of the mesh of 100×100 points where $\gamma = 15$, initially. The propagating front shown here coexists with the one shown in Fig. 5.

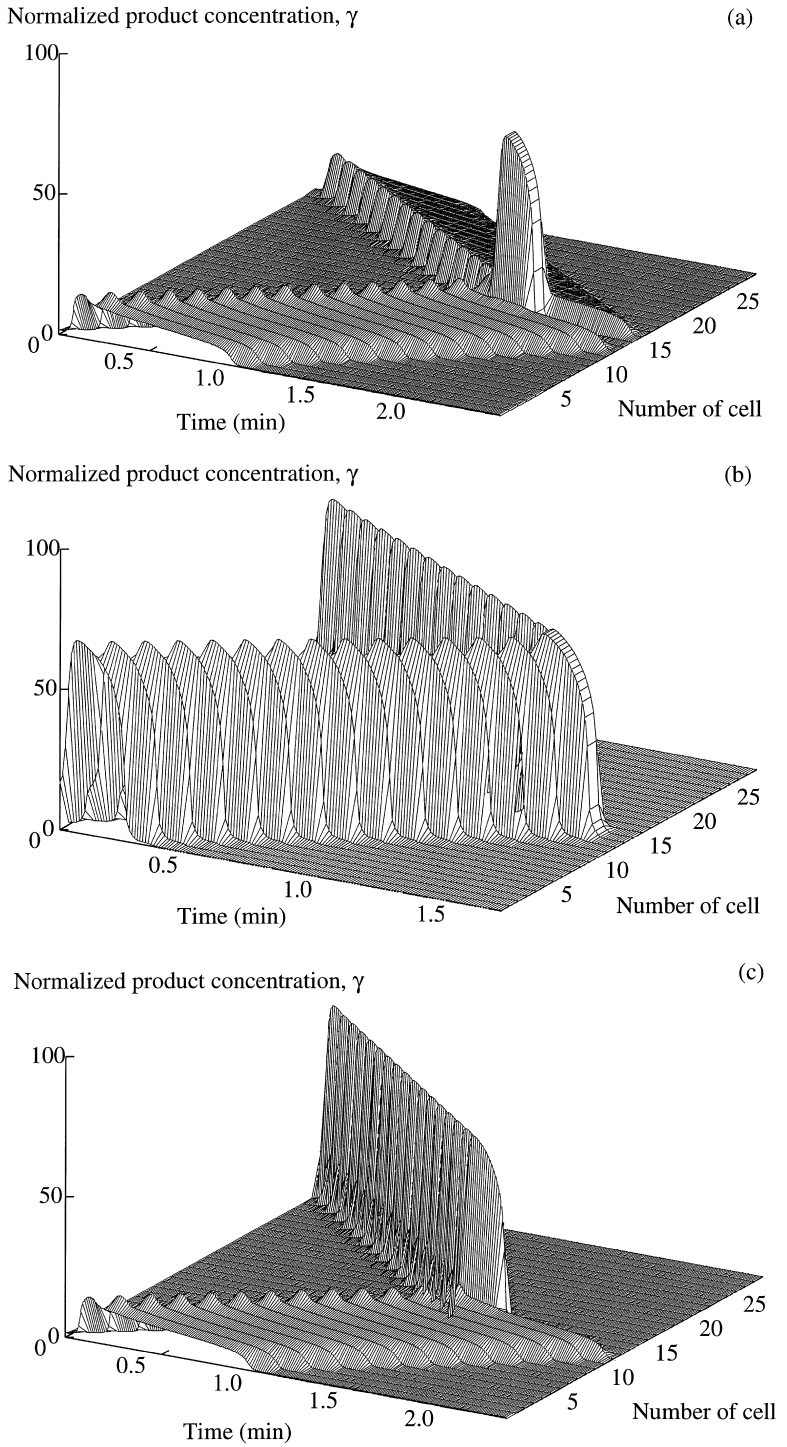

Fig. 7. Annihilation of two propagating wave-fronts upon collision. Two wave-fronts of small (a) or large (b) amplitude, started at the two extremities of the one-dimensional system, vanish upon collision. A similar phenomenon is observed (c) when a small-amplitude wave-front collides with a large-amplitude one. The conditions are those of Fig. 4.

been demonstrated [9–11]. The present results suggest that to observe a multiplicity of propagating wave-fronts, the most favorable conditions would correspond to those in which the steady state is stable but excitable beyond two distinct thresholds. Such multi-threshold excitability itself has not yet been demonstrated in chemical oscillatory systems displaying birhythmicity but, as suggested by phase plane analysis of the present model [15,16], the phenomenon should occur under closely related conditions.

Multi-threshold excitability is a property of thalamic neurons [26,27]. Other dynamic properties of these neurons are accounted for, in a qualitative manner, by the biochemical model considered here [28,29]. It is for thalamic neurons that the phenomena of birhythmicity and multiple wave-front propagation stand the best chances of being demonstrated experimentally. The coexistence of multiple periodic attractors has recently been reported in a theoretical study of a model neuron [14]. Interestingly, the propagation of two distinct action potentials has been observed experimentally in a neuronal preparation [30]; this observation may be taken as indicative of the type of multiplicity of spatiotemporal patterns reported in the present study. Multiple periodic states have also been reported in other neuronal preparations [31,32]. Thus it appears that neurobiology, together with chemistry, provides the best opportunities for demonstrating experimentally, in a given set of conditions, the coexistence of both multiple, simultaneously stable oscillatory regimes and multiple propagating waves.

Acknowledgements

This work was supported by the NATO collaborative research grant no. 0203/89 and by the program Actions de Recherche Concertée (ARC 94-99/180) launched by the Ministry of Education, French Community of Belgium.

References

[1] G. Nicolis, I. Prigogine, Self-Organization in Nonequilibrium Systems. From Dissipative Structures to Order through Fluctuations. Wiley, New York, 1977.
[2] H. Degn, Nature 217 (1968) 1047.
[3] I.R. Epstein, in: G. Nicolis, F. Baras (Eds.), Chemical Instabilities, D. Reidel, Dordrecht, 1984, p. 3.
[4] N. Minorsky, Nonlinear Oscillations, Van Nostrand, Princeton, NJ, 1962.
[5] R. Guttman, S. Lewis, J. Rinzel, J. Physiol. (Lond.) 305 (1980) 377.
[6] J. Jalife, C. Antzelevitch, Science 206 (1979) 695.
[7] O. Decroly, A. Goldbeter, Proc. Natl. Acad. Sci. USA 79 (1982) 6917–21.
[8] A. Goldbeter, Biochemical Oscillations and Cellular Rhythms. The Molecular Bases of Periodic and Chaotic Behavior. Cambridge University Press, UK, 1996.
[9] M. Alamgir, I.R. Epstein, J. Am. Chem. Soc. 105 (1983) 2500.
[10] P. Lamba, J.L. Hudson, Chem. Eng. Commun. 32 (1985) 369.
[11] O. Citri, I.R. Epstein, J. Phys. Chem. 92 (1988) 1865.
[12] M. Markus, B. Hess, Proc. Natl. Acad. Sci. USA 81 (1984) 4394.
[13] O. Decroly, A. Goldbeter, J. Theor. Biol. 124 (1987) 219.
[14] C.C. Canavier, D.A. Baxter, J.W. Clark, J.H. Byrne, J. Neurophysiol. 69 (1993) 2252.
[15] F. Morán, A. Goldbeter, Biophys. Chem. 20 (1984) 149.
[16] F. Morán, A. Goldbeter, Biophys. Chem. 23 (1985) 71.
[17] A.T. Winfree, Science 175 (1972) 634.
[18] M.J. Berridge, G. Dupont, Curr. Opin. Cell Biol. 6 (1994) 267.
[19] M.J. Berridge (Ed.), Ca^{2+} Waves, Gradients and Oscillations, CIBA Found. Symp., Wiley, Chichester, 1995.
[20] G. Dupont, A. Goldbeter, Biophys. J. 67 (1994) 2191.
[21] F. Alcantara, M. Monk, J. Gen. Microbiol. 85 (1974) 321.
[22] A. Goldbeter, R. Lefever, Biophys. J. 12 (1972) 1302.
[23] A. Goldbeter, Proc. Natl. Acad. Sci. USA 70 (1973) 3255.
[24] P. Maini, J. Math. Biol. 28 (1990) 307.
[25] S. Koga, Phys. Lett. A 191 (1994) 251.
[26] H. Jahnsen, R. Llinas, J. Physiol. (Lond.) 349 (1984) 205.
[27] M. Steriade, E.G. Jones, R.R. Llinas, Thalamic Oscillations and Signaling. Wiley Interscience, New York, 1990.
[28] A. Goldbeter, F. Moran, Eur. Biophys. J. 15 (1988) 277.
[29] R. Llinas, Science 242 (1988) 1654.
[30] B. Hochner, M.E. Spira, Brain Res. 398 (1986) 164.
[31] J. Hounsgaard, O. Kiehn, J. Physiol. (Lond.) 414 (1989) 265.
[32] E. Marder, L.F. Abbott, G.G. Turrigiano, Z. Liu, J. Golowasch, Proc. Natl. Acad. Sci. USA 93 (1996) 13481.